

The colouration toolkit of the Pipevine Swallowtail butterfly, *Battus philenor*: thin films, papiliochromes, and melanin

Doekele G. Stavenga · Hein L. Leertouwer ·
Bodo D. Wilts

Received: 16 December 2013 / Revised: 17 March 2014 / Accepted: 19 March 2014 / Published online: 9 April 2014
© Springer-Verlag Berlin Heidelberg 2014

Abstract The ventral hindwings of Pipevine Swallowtail butterflies, *Battus philenor*, display a colourful pattern, created by variously coloured wing scales. Reflectance and transmittance measurements of single scales indicate that the cream and orange scales contain papiliochrome pigments, while brown, black and blue scales contain melanin. Microspectrophotometry and scatterometry of both sides of the wing scales show that the lower lamina acts as a thin film, with reflection properties dependent on the scale's pigmentation. Notably in the orange scales, the reflectance spectrum of the lower lamina is tuned to the pigment's absorbance spectrum. The dorsal hindwings of the male (but not the female) *B. philenor* are blue-green iridescent. At oblique illumination, the light reflected by the male's dorsal hindwings can be highly polarised, which may have a function in intersexual signalling.

Keywords Wing scales · Microspectrophotometry · Scatterometry · Iridescence · Sexual signaling

Paper for a special issue of JCPA, celebrating the 100th anniversary of the publication of the paper by Karl von Frisch demonstrating honeybee colour vision.

D. G. Stavenga (✉) · H. L. Leertouwer · B. D. Wilts
Computational Physics, Zernike Institute for Advanced Materials,
University of Groningen, 9747 AG Groningen, The Netherlands
e-mail: d.g.stavenga@rug.nl

Present Address:

B. D. Wilts
Cavendish Laboratory, Department of Physics, University
of Cambridge, JJ Thomson Avenue, Cambridge CB3 0HE, UK

Introduction

Butterflies have attracted scientific interest since time immemorial, initially because of their colourful wings that intrigued the human observer (Kinoshita 2008), but in the last century also because butterfly vision has become well investigated (Arikawa 2003). Already Hooke recognised that insect vision relies on the multifaceted compound eyes, but he was astounded at how the tiny visual instruments of insects were able to perform their task (Hooke 1665). Much anatomical detail and optical insight were obtained in the nineteenth century (Exner 1891), but a major breakthrough in insect vision research was achieved by Karl von Frisch, who published 100 years ago his pioneering, behavioural work on colour vision of the European honeybee, *Apis mellifera* (von Frisch 1914). Insect colour vision has since been a central theme in insect biology. Electrophysiological and behavioural studies unequivocally demonstrated that bees have trichromatic vision (Menzel and Backhaus 1989), and as this also holds for humans, this was for a long time expected to be the case for insects in general. In the recent decades, this view has become modified, particularly for the papilionid butterfly *Papilio xuthus*, which perceives the colourful world with a tetrachromatic colour vision system (Kinoshita et al. 1999; Koshitaka et al. 2008).

In addition to his pioneering work on bee colour vision, Karl von Frisch also opened up the field of polarisation vision by his discovery that polarised light plays a principal role in bee vision, specifically in navigation (von Frisch 1949). Polarisation vision has since played a central role in visual studies of arthropods. For instance, recent research has shown that butterflies also have well-developed polarisation vision (Bandai et al. 1992; Kelber et al. 2001; Sweeney et al. 2003; Kinoshita et al. 2011).

Here, we investigate the spectral and polarisation properties of the wings of Pipevine Swallowtails, *B. philenor*, strikingly coloured butterflies, common in the southern US states and Mexico, and their relationship with butterfly vision. The butterflies are aposematic, because the caterpillars feed on plants in the chemically defended genus *Aristolochia*, thus accumulating abundant aristolochic acids, which makes the butterflies unpalatable for bird predators. The colouration of the butterfly is of particular interest, because the species is at the centre of a mimicry complex shared by a number of other papilionid as well as nymphalid butterfly species (Brower 1958; Brower and Brower 1962). The mimicked pattern is that of the ventral hindwings, displayed when resting with closed wings, which consists of a main, metallic blue field dotted with orange, cream and white patches (Rutowski et al. 2010; Pegram et al. 2013a).

Several studies have been devoted to the biology of *B. philenor*'s colouration, especially its role in mimicry and signalling (Pegram et al. 2013b; Rajyaguru et al. 2013; Rutowski and Rajyaguru 2013). Less attention has been devoted so far to the optical basis of the colours, which essentially reside in the wing scales that cover the wing substrate like tiles on a roof. As holds generally for butterfly wings, the packing of the scales on the wing membrane, their pigmentation, and their fine-structure together determine the colouration (Srinivasarao 1999; Stavenga et al. 2006a; Kinoshita 2008; Kinoshita et al. 2008). A butterfly wing scale basically consists of two layers of cuticle, the upper and lower laminae, which are connected by pillars, the trabeculae (Ghiradella 1998, 2010). The space between the lower and upper lamina, the lumen, is in many scales virtually empty, but the lumen sometimes is filled with layered or intricate three-dimensional structures (Ghiradella 1984). Whereas the lower lamina is usually relatively flat, the upper lamina is highly structured, with rows of parallel ridges (typical interdistance 1–2 μm) covered by overlapping lamellae. On the ridge slopes, parallel microribs (interdistance $\sim 0.2 \mu\text{m}$) run perpendicular to the ridge direction. Most of the microribs are commonly interrupted, and those remaining form the so-called crossribs, which frame more or less open windows to the scale lumen.

As is usual in colour studies, butterfly wing colours are classified as structural and pigmentary. Structural colours predominate when the scale has regular, periodic-spaced elements, with distances in the submicrometer range. The most well-known examples are the brightly blue-reflecting *Morpho* butterflies, which have scales whose ridges bear lamellae that function as optical multilayers (Vukusic et al. 1999; Kinoshita et al. 2002). A similar structural organisation exists in various butterfly species in families other than the nymphalids, for instance pierids (Ghiradella et al. 1972; Stavenga et al. 2006; Rutowski et al. 2007; Ingram and Parker 2008), riodinids (Vukusic et al. 2002) and lycaenids

(Tilley and Eliot 2002; Biró et al. 2007; Wilts et al. 2009). The blue lycaenids have in the lumen of the blue scales a multilayer that reflects in the blue wavelength range (Wilts et al. 2009; Bálint et al. 2012). Other lycaenids have scales with gyroid structures acting as 3D photonic crystals, reflecting blue and yellow, resulting in a greenish colour (Michielsen and Stavenga 2008; Michielsen et al. 2010). Similar 3D structures occur in some papilionids (Vukusic and Sambles 2003; Wilts et al. 2012a).

When the scale structures are irregularly arranged, incident light is scattered randomly. In the absence of pigment, the scales are white (e.g. Stavenga et al. 2010). However, when a scale contains a pigment, it becomes coloured depending on the pigment's absorption spectrum. Actually, when the pigment absorbs exclusively in the ultraviolet, the scale remains white for a human observer but it is coloured in the eyes of butterflies. With absorption spectra extending into the human visible wavelength range, distinct pigmentary colourations occur that are visible to both butterflies and humans. Melanin pigments, creating brown to black, are encountered universally in butterfly wings, but the various butterfly families express in addition characteristically different pigment classes. For instance, ommochromes and their precursor kynurenine create the red and yellow colours of nymphalids (Nijhout 1991, 1997; Reed and Nagy 2005). Similarly, in papilionids various papiliochromes yield yellow, orange or red (Umebachi 1985; Koch and Behnecke 2000; Wilts et al. 2012b). The melanins, ommochromes and papiliochromes are distributed throughout the wing scale's structural components, but in the wing scales of pierid butterflies, pterin pigments are concentrated in granular beads, attached to the crossribs. The beads function as short-wavelength absorbing, long-pass filters as well as effective light scatterers, thus causing bright-white, yellow, orange or red-coloured wing scales (Stavenga et al. 2004; Rutowski et al. 2005; Stavenga et al. 2006; Morehouse et al. 2007; Wijnen et al. 2007). In some scattered butterfly cases, flavonoids, carotenoids, and bile pigments have been demonstrated, specifically in the wing membrane (Nijhout 1991; Stavenga et al. 2010).

Many butterfly wing scales are coloured by both structural and pigmentary methods. A clear example is the *Papilio nireus* group. The wings of these butterflies have conspicuous blue-green bands surrounded by black margins. The lower lamina of the scales in the coloured wing areas is a thin film, reflecting broad-band blue light. The upper lamina is a thick meshwork of crossribs that contains the violet-absorbing pigment papiliochrome II. The upper lamina thus acts as an optical band-filter, limiting the reflected light to the blue-green wavelength range (Trzeciak et al. 2012; Wilts et al. 2012b).

Melanin pigment has often a contrast enhancement function. For instance, in *Morpho* wing scales, the melanin

deposited below the multilayered ridges effectively absorbs transmitted light, which potentially could be scattered back by the wing or other scale structures. The melanin thus enhances the saturation of the colour signal (Mason 1924; Kinoshita et al. 2008). In a different way, in several pierid butterflies, the ridge interference reflectors create an enhanced chromatic signal, which increases contrast and/or visibility, because they contribute to the reflectance in the short-wavelength range, where the wing pigments strongly absorb (Stavenga et al. 2004; Rutowski et al. 2005; Stavenga et al. 2006; Morehouse et al. 2007; Pirih et al. 2011; Wilts et al. 2011).

To unravel the various components and optical mechanisms that determine the colouration of *B. philenor* wings, we have performed (micro)spectrophotometry, (electron) microscopy, scatterometry, and optical modelling. We thus found that the blue iridescent colour of the ventral hindwing scales has clearly a structural basis, whilst the orange spots have a pigmentary colour. Our measurements of the reflection properties of the two sides of single scales, taken from the different wing areas, indicate that the various colours result from unique combinations of thin-film reflectors and papiliochrome or melanin pigments.

Of specific interest is that the two sexes of *B. philenor* exhibit a strong sexual dichromatism (Rutowski et al. 2010; Rutowski and Rajyaguru 2013). The dorsal hindwings of males are blue-green iridescent. The light reflected by the iridescent hindwings can be distinctly polarised, depending on the angle of light incidence, which may play an important role in intersexual signalling.

Materials and methods

Animals

Wings of *B. philenor* butterflies, glued to black cardboard, as well as intact butterflies were obtained from a colony maintained by Kimberly Vann Pegram and Ronald Rutowski (School of Life Sciences, Arizona State University). Butterflies were also supplied by Ric Wehling (Eglin AFB).

Photography

The male *B. philenor* of Fig. 1 was photographed in the butterfly collection of the National History Museum Naturalis (Leiden, curator Dr R. de Jong) with a Nikon D70 camera, which was also used for photographing the male and female dorsal hindwings (Fig. 6a, b). Photographs of single scales, obtained by gently pressing the wings onto a microscope slide, in immersion fluid (refractive index 1.60 at 586 nm; Figs. 2, 6c, d) were made with a Zeiss

Universal Microscope (Zeiss, Oberkochen, Germany) using a Nikon Fluor 40/1.30 oil objective (Nikon, Tokyo, Japan); the digital camera was a Kappa DX-40 (Kappa Optronics GmbH, Gleichen, Germany). For the photograph of a local wing area, an Olympus 10/0.30 objective was used (Olympus, Tokyo, Japan; Fig. 3a). For the photograph of an orange scale (Fig. 3b), a dark field Zeiss Epiplan 80/0.95 objective and for that of a blue scale (Fig. 3c) a bright field Epiplan 40/0.85 objective were used. Photographs of both the adwing (lower) side and abwing (upper) side of single scales glued to a glass micropipette (Fig. 4) were made using a Zeiss Epiplan16, 0.35 objective. Photographs of the dorsal hindwing scales (Fig. 6c, d) were made with an Olympus SZX16 stereomicroscope equipped with an Olympus DP70 digital camera.

Spectroscopy

Reflectance spectra of different wing areas (Fig. 1c) were measured with a bifurcated probe (Avantes FCR-7UV200; Avantes, Eerbeek, Netherlands), using an AvaSpec 2048-2 CCD detector array spectrometer (Avantes, Eerbeek, Netherlands). The light source was a deuterium-halogen lamp (AvaLight-D(H)-S). The bifurcated probe, positioned normally to the wing surface, illuminated an area with a diameter of about 1 mm and captured the light reflected in a small spatial angle, aperture about 20°. The reference was a white diffuse reflectance tile (Avantes WS-2), and thus non-diffusively reflecting wing parts could yield relative reflectance values larger than 1. The white diffuse reference was also used in the measurements of the reflectance spectra of both sides of single scales attached to a glass micropipette, which were performed with a microspectrophotometer (MSP; Fig. 4). The MSP consisted of a Leitz Ortholux microscope (Leitz, Wetzlar, Germany) connected to the detector array spectrometer, with a xenon arc lamp light source. Absorbance spectra of single scales immersed in refractive index fluid were also measured with the MSP (Fig. 2). The area measured with the MSP was rectangular with sides typically ~15 µm. The microscope objective was an Olympus LUCPlanFL N 20x, 0.45 (Olympus, Tokyo, Japan). Due to the glass optics, the MSP spectra were limited to wavelengths >350 nm. To determine the absorption properties of cuticle at shorter wavelengths, we used two opposed optical fibres with the deuterium-halogen light source and the detector array spectrometer and measured the spectral transmittance of a wing piece of a cicada (probably *Cicochila australasiae*), which has clear wings without scales (Fig. 5a). The thickness was derived from reflectance measurements using thin-film theory (Stavenga et al. 2012b) and the known refractive index (Leertouwer et al. 2011). This allowed calculation of the absorption coefficient.

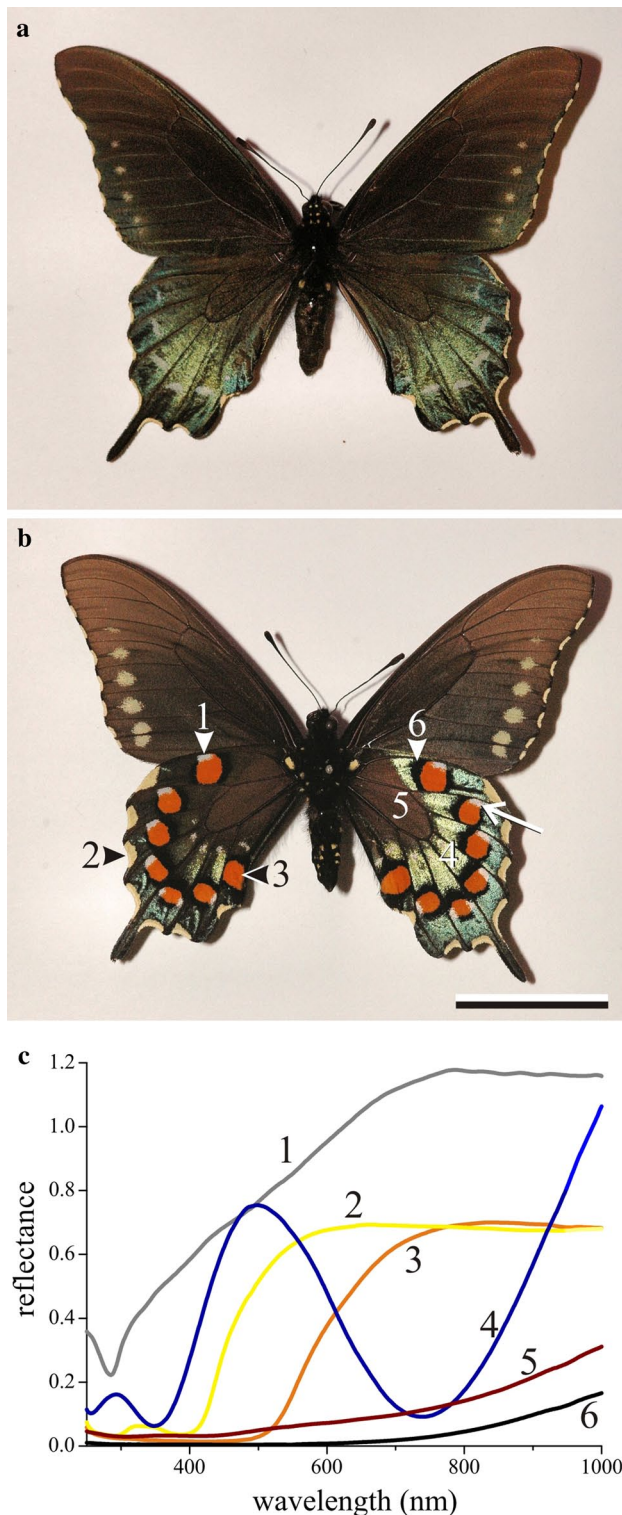


Fig. 1 A male Pipevine Swallowtail. **a** Dorsal view, showing the brown forewings and the *blue* iridescent dorsal hindwings, with *whitish* areas and *cream-coloured* crescents. **b** Ventral view, showing *brown* forewings with *creamy* spots, and hindwings, which also have a *brown* area, but mostly feature a *bright blue* iridescent area (4), together with *orange spots* (3), bordered by *black* (6) and *white* (1) areas, and *cream-coloured* (2) crescents at the wing margins; scale bar **a**, **b** 2 cm. The arrow points to the area where Fig. 3a was taken. **c** Reflectance spectra measured from the numbered areas in **b**

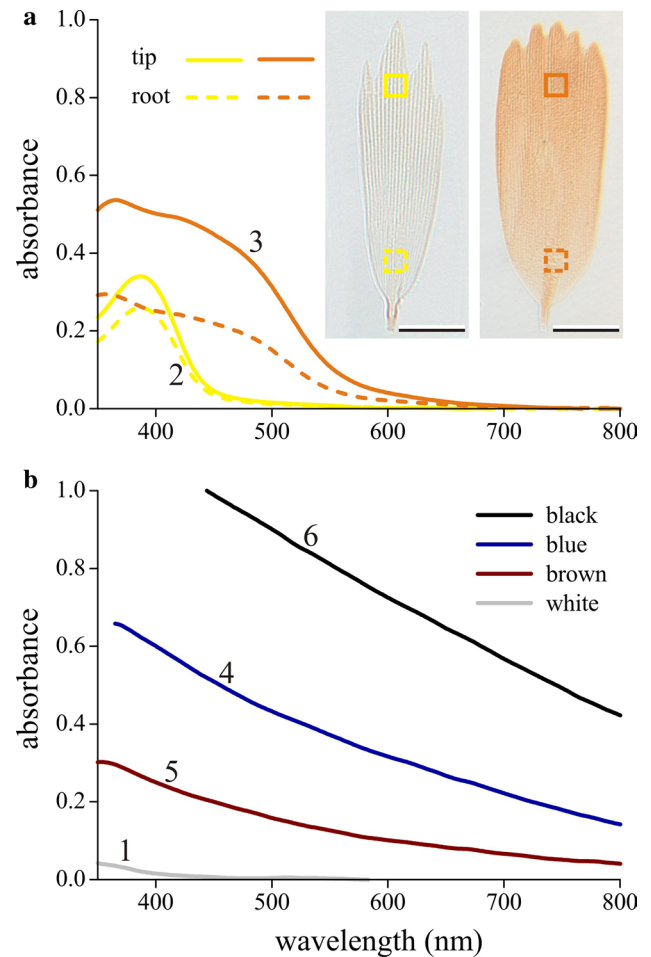


Fig. 2 Absorbance spectra measured from single scales, taken from the numbered areas of Fig. 1b. **a** Absorbance spectra of a *cream-coloured* (Fig. 1b, #2; inset, left scale) and an *orange* (Fig. 1b, #3; inset, right scale) wing scale, measured from the tip (solid curves; inset, solid squares) and root (dashed curves; inset, dashed squares) areas. Scale bar (insets): 50 μm . **b** Absorbance spectra measured from a *black*, *blue*, *brown*, and *white* scale (Fig. 1b, #6, 4, 5, and 1, respectively)

Scanning electron microscopy (SEM)

A scanning electron microscope (Philips XL-30 ESEM; Philips, Eindhoven, The Netherlands) was used to visualise the scale anatomy (Fig. 3d, e). Prior to imaging, the samples were sputtered with palladium.

Imaging scatterometry

For investigating the spatial reflection characteristics of the wing scales, we performed imaging scatterometry (Stavenga et al. 2009; Vukusic and Stavenga 2009; Wilts et al. 2009). An isolated, single scale attached to a glass micropipette (Fig. 4) or a wing patch (Fig. 7) was positioned at the first focal point of the ellipsoidal mirror of the imaging scatterometer. The

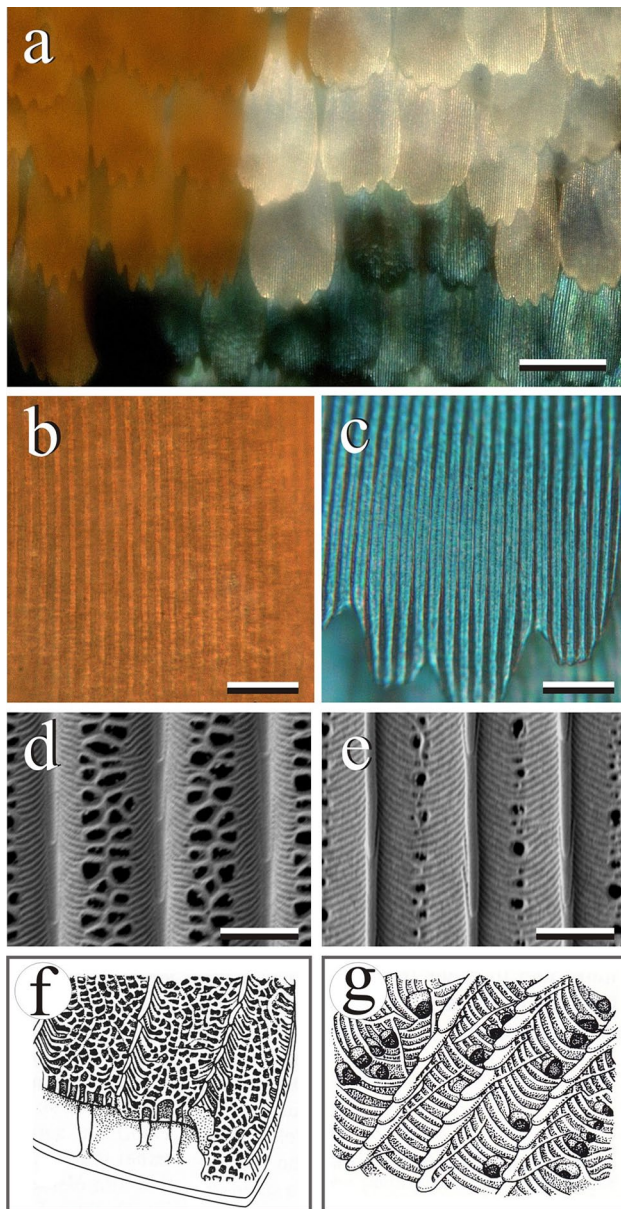


Fig. 3 Structure of various *Battus philenor* wing scales. **A** Photograph of a small area of the ventral hindwing, with orange, white, blue and black scales (indicated by the arrow in Fig. 1b). **b** Epilumination light microscopy of an orange scale. **c** A blue scale with in between the ridges bright-blue reflecting areas with central rows of small, dark dots. **d** Scanning electron microscopy (SEM) of an orange scale, showing ridges with slightly overlapping lamellae and crossribs creating irregularly shaped windows. **e** SEM of a blue scale with microribs leaving very small windows. **f**, **g** Two of the scale types classified by Ghiradella (1998, 2010). Scale bars **a**: 100 μm ; **b**, **c**: 10 μm ; **d**, **e**: 2 μm

scatterograms were obtained by focusing a white light beam with a narrow aperture ($\sim 5^\circ$) at a small circular area (diameter $\sim 13 \mu\text{m}$) of the isolated scale, and the spatial distribution of the far-field scattered light was then monitored. A flake of magnesium oxide served as a white diffuse reference object.

Polarisation- and angle-dependent reflectance measurements

The angle- and polarisation-dependence of the reflectance spectra of the male dorsal hindwing was measured using two optical fibres (Fig. 8). One end of the first optical fibre was connected to a xenon lamp, and its other end was mounted at a goniometer together with a small lens, which focused the fibre tip at the goniometer's rotation axis. At a second goniometer one end of the second fibre was mounted with additionally a focusing lens and a polarisation filter, which could be rotated around the optical axis of lens and fibre entrance; the other end of the fibre was connected to the CCD detector array spectrometer. The rotation axes of the two goniometers coincided and the two fibre tips rotated in the same plane. The wing patch to be measured was positioned in that plane, at the axis of rotation of the goniometers. The aperture of the fibres was 5° (full width at half maximum of the far-field radiation pattern), and the distance of the tips to the centre of the illuminated spot was 4 and 12 cm, respectively. The receiving fibre thus sampled a larger area than the illuminated spot (but it did not fully capture all the reflected light). The white diffuse reflectance tile (Avantes WS-2) served as reference.

Calculations of thin-film reflectance spectra

For calculating the reflectance of a single thin film (Fig. 5b, c), we used the Airy formulae, as before (Stavenga et al. 2012b). For the calculations of the reflectance of a multilayer consisting of three thin films (Fig. 5c), we used a matrix formalism (Stavenga et al. 2011).

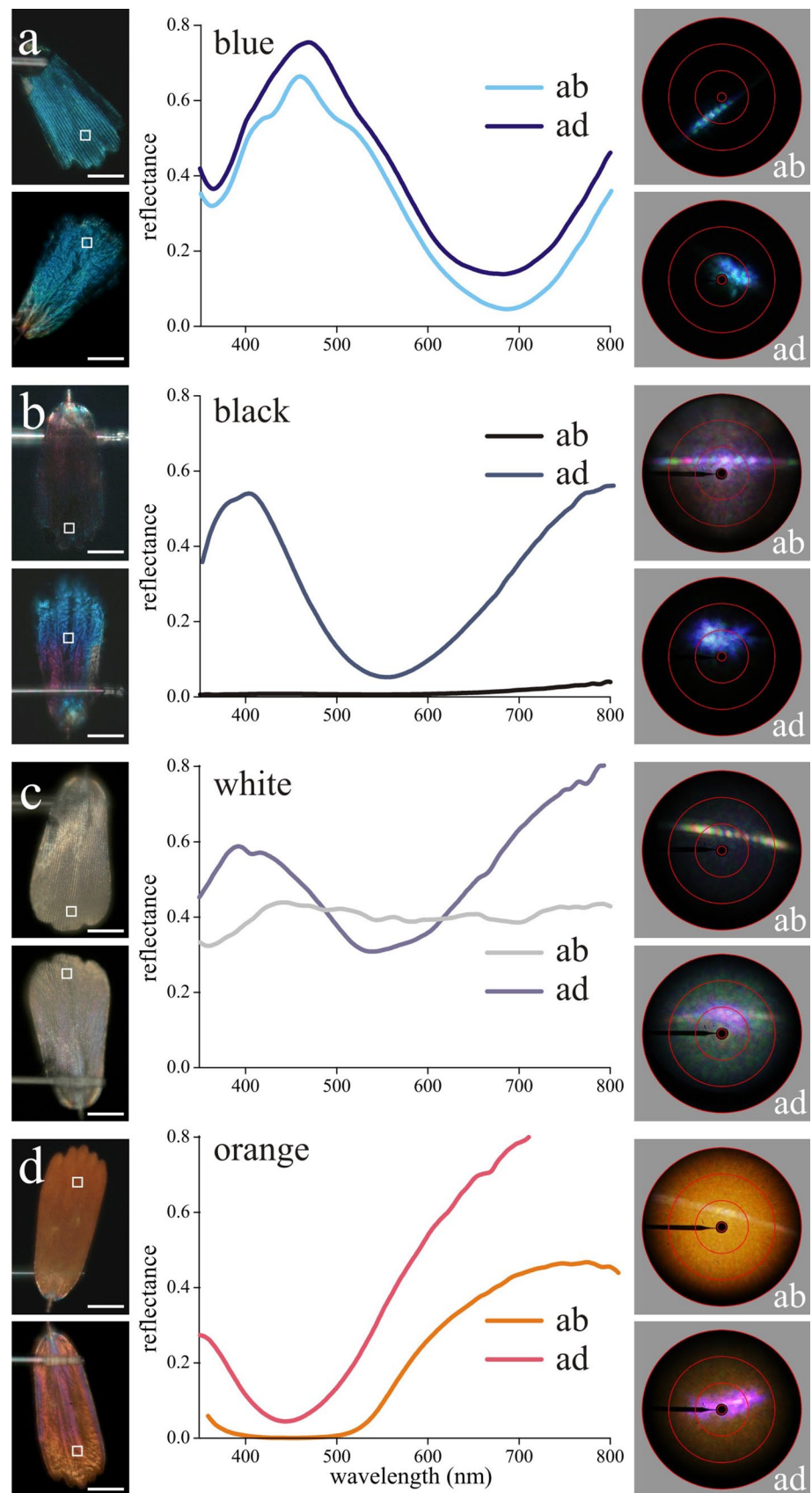
Results

Colour and reflectance spectra of *B. philenor* wings

Both dorsal (upperside) and ventral (underside) hindwings of the male Pipevine Swallowtail butterfly have a main bluish-metallic reflection, whereas the forewings are dark-brown to black (Fig. 1). The ventral hindwings are strikingly marked by a curved row of prominent submarginal orange spots, which are flanked by black and white areas. The ventral hindwings are fringed by cream crescents (Fig. 1b). The forewings are dotted with similar cream-coloured spots (Fig. 1a, b).

We measured reflectance spectra from the various coloured areas with a bifurcated probe (Fig. 1c); the spectra's number corresponds to the numbered area in Fig. 1b. In the cream and orange wing patches, the reflectance is low at short wavelengths and high at long wavelengths, which is characteristic for light scattering media containing

Fig. 4 Optics of single ventral hindwing scales (male). *Left-hand column* photographs of abwing (*top*) and adwing (*bottom*) sides of a blue (**a**), black (**b**), white (**c**), and orange scale (**d**); scale bars 50 μm . *Middle column* reflectance spectra measured from a small area, indicated by the *white square* in the photographs of the left-hand column. *Right-hand column* scatterograms of a small area in the ab- and adwing sides of the four scales. The *circles* indicate scattering angles of 5°, 30°, 60°, and 90° (see Fig. 7b)



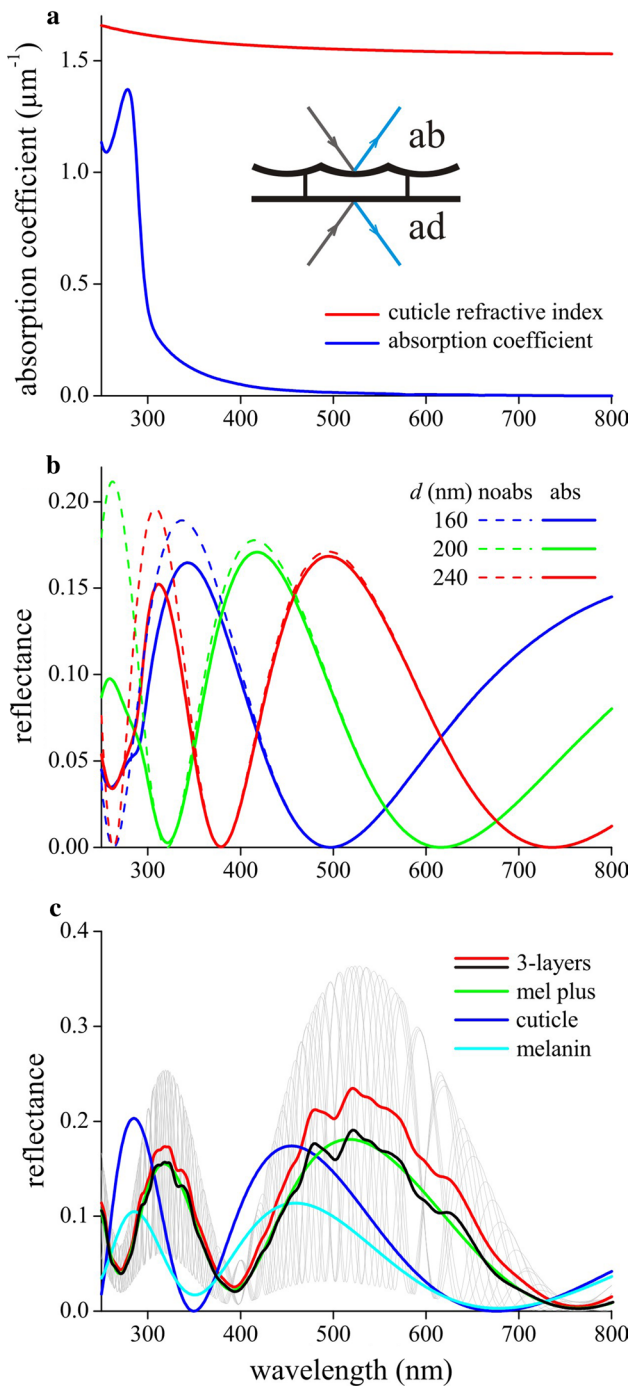


Fig. 5 Thin film optics of blue/green scales. **a** Refractive index of the scale cuticle and its associated absorption coefficient. *Inset:* diagram of a blue scale, consisting of a flat lower lamina and a curvy upper lamina, which are connected by trabeculae. **b** Reflectance spectra of a single thin film, consisting of chitin, with thicknesses 160, 200 and 240 nm. The dashed curves hold for thin films made of cuticle with refractive index as given in **a**, but neglecting absorption. The continuous curves are obtained when absorption is taken into account, assuming an absorption coefficient as given in **a**. **c** Reflectance spectra for a thin film cuticle with thickness 220 nm, with the refractive index and absorption coefficient of **a** (blue curve chitin); for the same thin film, but containing melanin with half of the absorbance of the blue scale of Fig. 2b (cyan curve melanin); for the latter thin film but with an 0.2 higher refractive index (green curve mel plus); for two of the latter thin films separated by an air gap at a distance 1.0, 1.1, 1.2,...2.0 μm (grey spectra), yielding as the average reflectance spectrum the red curve (3 layers). Calculation of the reflectance as the average electric field amplitude squared yielded the black curve

1.6, which approximates the refractive index of butterfly scales (Leertouwer et al. 2011; Stavenga et al. 2013), and then measured the absorbance spectra at various locations of the scale (Fig. 2). The absorbance spectra of one and the same scale have always the same shape, but the amplitude gradually decreases from the scale tip to the scale root (Fig. 2a). The pigment of the cream scales absorbs mainly in the (ultra)violet and has a peak absorbance at 387 nm (Fig. 2a). The spectrum closely matches that of papiliochrome II, which was first identified in another papilionid butterfly, the Japanese Yellow Swallowtail, *Papilio xuthus* (Umebachi 1985; Wilts et al. 2012b). The absorbance spectrum of the pigment in the orange scales of *B. philenor* peaks also in the ultraviolet, but it extends to much longer wavelengths than papiliochrome II (Fig. 2a).

Not surprisingly, the absorbance of the white scales appears to be very minor above 400 nm (Fig. 2b). Nevertheless, the reflectance of the white area (Fig. 1c, #1) in the far-ultraviolet (<300 nm) is very low, which must be due to chitin, the basic material of the scales and wings of *B. philenor*, like in the wings and cuticle of other insects (see below). Evidently, when the scales are additionally filled with the pigments of Fig. 2a, the long-pass spectra of the cream (Fig. 1c, #2) and orange scales (Fig. 1c, #3) result.

The absorbance spectra of the black, blue, and brown scale have a similar shape, clearly revealing the presence of melanin (Fig. 2b). The reflectance spectra of the corresponding wing areas are quite different, however. The wing areas with brown scales have a higher reflectance than the black areas (Fig. 1c, #5 and #6), which can be readily understood from the brown scales' lower absorbance (Fig. 2b). The absorbance of the blue scales is in between those of the brown and black scales (Fig. 2b), and thus a reflectance spectrum of the blue wing area in between those of the brown and black wing areas might have been expected, but the actually measured reflectance spectrum is completely different (Fig. 1c, #4). This suggested that the

short-wavelength absorbing pigments, which thus act as long-pass optical filters. In all wing areas, the reflectance in the ultraviolet is minor, except perhaps in the very small white patches.

Pigmentation of the wing scales

To investigate the nature of the pigments present in the scales, we isolated single scales from the various wing areas, embedded them in a medium with refractive index

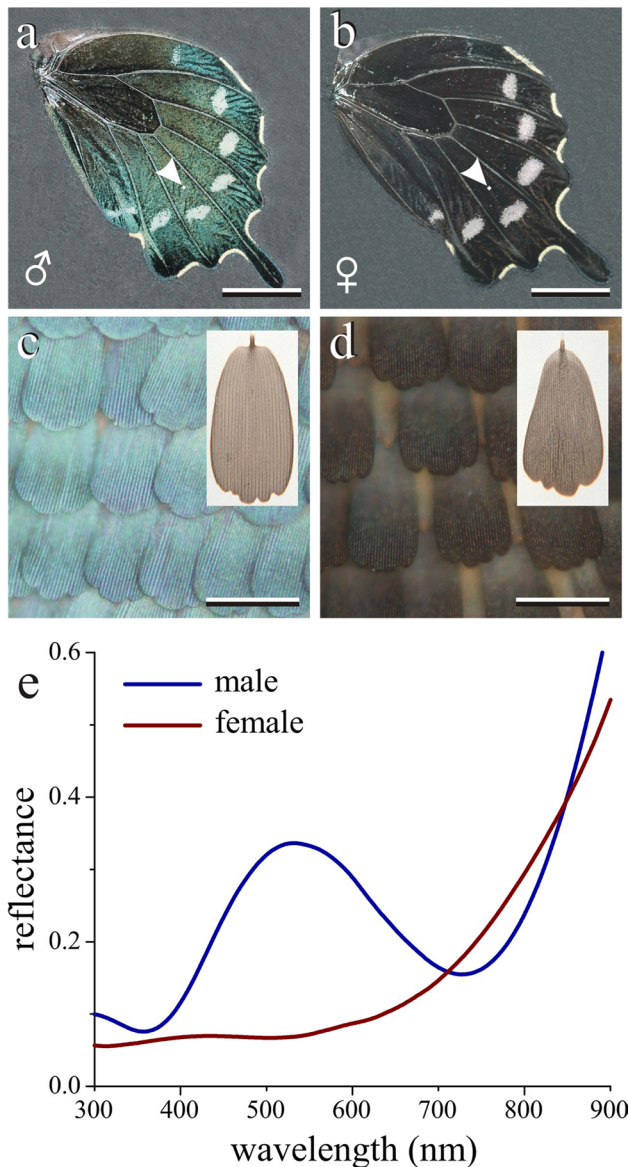


Fig. 6 Sexual dimorphism of the dorsal hindwings. **a, b** Photographs of the dorsal hindwings of a male and female *B. philenor* glued to black cardboard. **c, d** Close-up views of the male and female wings indicated in **a** and **b** by the small dot in front of the arrowhead. Insets: scales immersed in a fluid with refractive index 1.60 observed with transmitted light. **e** Reflectance spectra of the wings measured near the arrowheads in **a** and **b** with a bifurcated probe. Scale bars **a, b**: 1 cm; **c, d**: 100 μm

blue colour must have a structural basis, which we, therefore, further investigated.

Scale structure

To uncover possible differences in scale structure, we applied incident light and scanning electron microscopy (Fig. 3). We thus encountered in *B. philenor* two of the seven main classes of butterfly scale types distinguished by Ghiradella

(1998, 2010). The abwing (upper) surface, i.e. the surface of the upper lamina, always features parallel ridges (Fig. 3b, c), consisting of slightly overlapping lamellae, with microribs running perpendicularly to the ridges (Fig. 3d, e). In all scales except the blue ones (Fig. 3e), the microribs leave irregularly shaped open windows (Fig. 3d). The size of the windows somewhat varies between the different coloured scales. The windows of the blue scales' upper lamina are very small (see Ghiradella 1985), which apparently has a profound effect on the scale's reflectance properties.

The adwing (lower) surface, i.e. the surface of the lower lamina, is generally rather smooth with slight wrinkles, as is well-known to hold for most butterfly wing scales (Ghiradella 1998; not shown).

Dependence of the spectral reflectance on scale structure and pigmentation

To learn how the pigmentation, structure and reflection characteristics of the various scales are related, we isolated single scales from the various coloured wing areas, mounted them on a glass micropipette and measured from both the abwing and adwing surface the reflectance spectra, using a microspectrophotometer. The rationale for investigating both scale surfaces was the question to what extent the lower lamina contributes to the total scale reflectance when the scale is illuminated from above in the normal, in situ situation.

Figure 4 shows the results for a blue (Fig. 4a), a black (Fig. 4b), a white (Fig. 4c), and an orange (Fig. 4d) scale, in the left-hand column photographs of the ab- and adwing surface and in the middle column reflectance spectra. The small squares in the photographs indicate the areas where the reflectance spectra were measured.

The blue scale has a blue-metallic appearance at both sides (Fig. 4a). The shape of the reflectance spectra unequivocally indicates thin-film reflection (see further below). The black scale's abwing side is, indeed, black, with minimal reflectance (Fig. 4b), clearly due to the high melanin absorbance (Fig. 2b). The adwing side shines metallic, in agreement with the measured reflectance spectrum (Fig. 4b). Colour and reflectance spectrum somewhat depend on the location, indicating that the lower lamina is an optical thin film with slightly varying thickness. The white scale's abwing side is dull-white, and the reflectance is substantial at all wavelengths (Fig. 4c), in agreement with the absence of an absorbing pigment (Fig. 2b). Locally at the adwing side a blue sheen is visible, indicating that the lower lamina of the white scale also acts as a thin film. Reflectance spectra measured from different areas of the white scale's adwing side resemble those measured at the abwing side. This suggests that in both cases light scattering by the ridges and crossribs as well as thin-film reflections by the lower lamina contribute to the reflectance

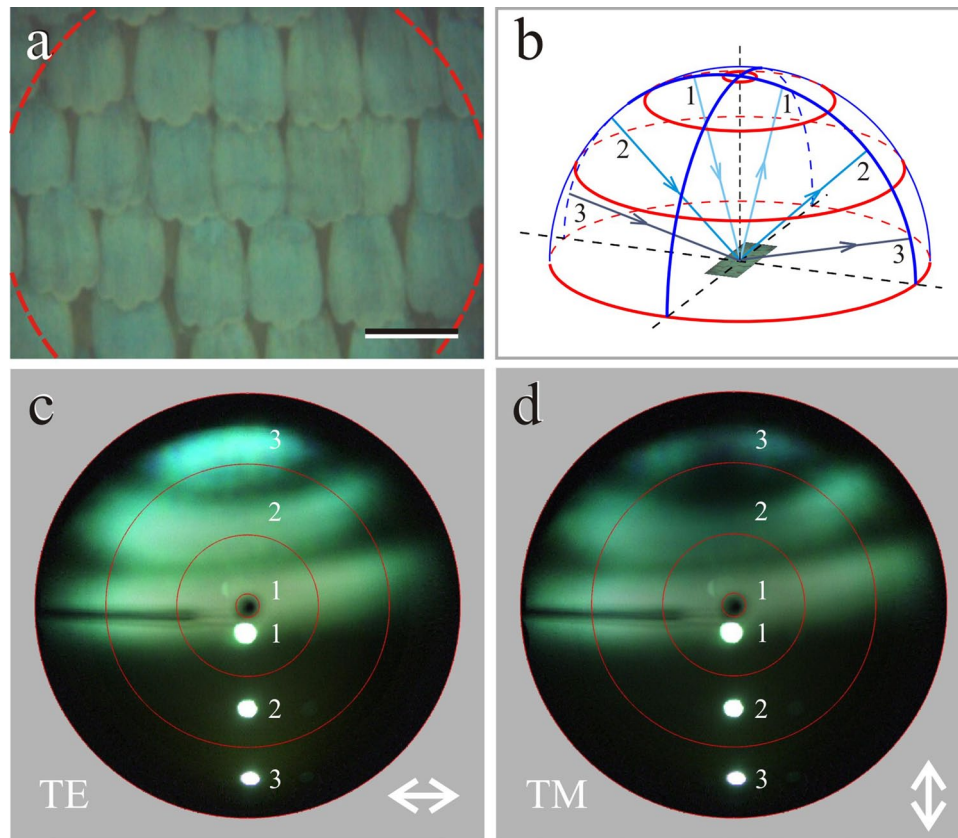


Fig. 7 Imaging scatterometry of a wing piece from the dorsal hindwing of a male *Battus philenor*. **a** A spot with diameter about $530\ \mu\text{m}$, indicated by the red circle, is illuminated; scale bar $100\ \mu\text{m}$. **b** Diagram of the reflection by the wing piece from inclination angles 15° , 45° , and 75° (#1, 2, 3, respectively). If the wing acts as a mirror, the reflected beams have the same inclination angles as the incident light beams. The red circles represent angular directions with inclination angles of 5° , 30° , 60° , and 90° . These directions are

shown as red circles in the polar plots of **c** and **d**. **c** Superimposed scattering patterns obtained with narrow aperture ($\sim 10^\circ$) beams of polarised white light incident from three directions, with inclination angles about 15° , 45° , and 75° (beam 1, 2, and 3, respectively, indicated by white dots). The TE-polarised light creates patterns 1, 2, and 3, respectively. **d** Superimposed scattering patterns obtained with TM-polarised light, incident from the same angles as in **c**. The black shadow at 9 o'clock is due to the glass pipette holding the wing piece

signal. Finally, the orange scale has abwing a dull orange colouration, clearly due to the short-wavelength-absorbing pigment identified in Fig. 2a, which causes a low reflectance at short wavelengths and leaves a high reflectance at long wavelengths (Fig. 4d). Observation of the adwing side shows a metallic reflection, varying from golden to purplish, again indicating thin-film optics, but the thin film must be quite different from those of the other scales. Compared to the other scales, the reflectance spectrum is shifted $\sim 100\ \text{nm}$ towards shorter wavelengths, which suggests an appreciable lower thickness, as follows from the analysis below (section Thin films).

Spatial distribution of scattered light by the wing scales of *B. philenor*

The reflectance spectra of Fig. 4 (middle column) were measured with a microspectrophotometer via an objective

with a limited aperture, which thus captures only part of the reflected light. To study the angular distribution of the scattered and reflected light in the full hemisphere above the scales' surface, we applied imaging scatterometry. A narrow aperture, white light beam illuminated a small area in the middle of the scale shown in the photographs in the left hand column. This yielded the scatterograms of Fig. 4, right-hand column.

The scatterogram of the abwing side of the blue scale (Fig. 4a) is a blue-coloured dotted pattern, resembling a diffraction pattern. The upper lamina of the blue scale is a blue-reflecting layer interrupted by an array of longitudinal ridges (Fig. 3c), which will cause a blue diffraction pattern oriented perpendicular to the ridges. The scatterogram of the adwing side of the blue scale is a blue fuzzy spot. Clearly, the lower lamina acts as a blue-reflecting thin film, but because it is not perfectly flat (see the adwing photograph), the reflected light is slightly spread out.

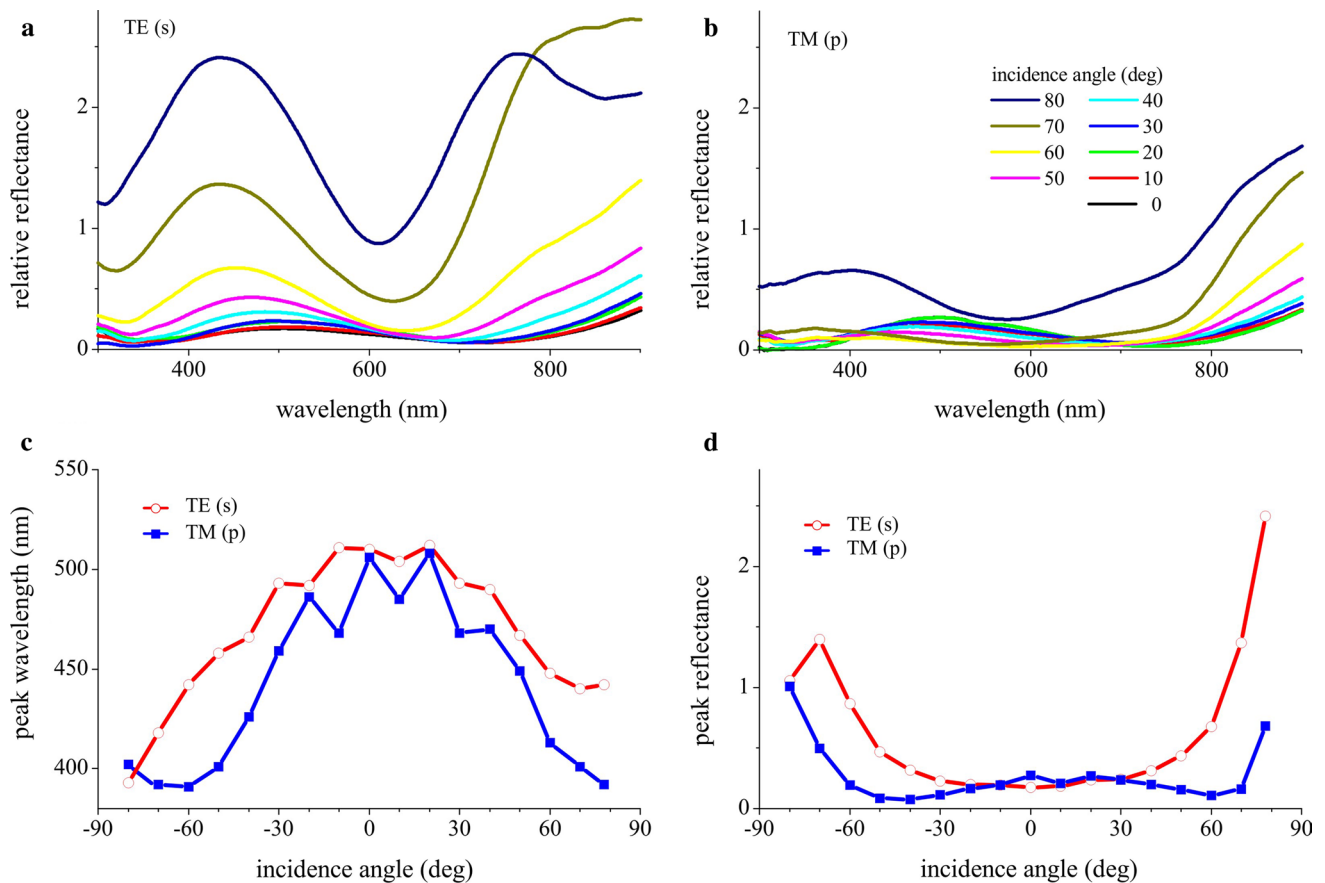


Fig. 8 Angle and polarisation dependence of the light reflection of the male dorsal hindwings. **a** Reflectance spectra measured as a function of the angle of light incidence for TE-polarised light. **b** Reflec-

tance spectra for TM-polarised light. **c** Peak wavelengths of the reflectance spectra. **d** Peak reflectance of the spectra for TE- and TM-polarised light

In the black scale's abwing scatterogram (Fig. 4b), diffraction is prominent, but also wide-field scattering is visible. We have to note here that the scatterogram was obtained with a long exposure time, because the reflection intensity was very minor (as shown by the minimal abwing reflectance spectrum). Quite in contrast is the adwing scatterogram, which is again a fuzzy blue spot, clearly due to the lower lamina's (slightly wrinkled) thin film.

The scatterogram of the white scale's abwing surface features a distinct, spatially extended coloured line (Fig. 4c), demonstrating that the scale ridges acted as a reflection grating. Wide-field scattered light can be additionally recognised. The scatterogram of the white scale's adwing surface shows in the centre a bluish, fuzzy spot, which must represent thin-film reflections from the lower lamina. Additionally, a diffraction pattern can be seen, which must be due to light that had passed the scale's lower lamina and was subsequently reflected by the scale's upper lamina, where the ridges again acted as a reflection grating. Furthermore, there is wide-field scattered light, which must be due to scattering by the scale components, i.e. the

crossribs and the trabeculae that connect the upper and lower lamina.

The scatterogram of the abwing side of the orange scale (Fig. 4d) also shows a diffraction pattern, but here wide-field, orange-coloured scattered light dominates, undoubtedly emerging from the irregular arranged structures in the upper lamina and the trabeculae. The adwing scatterogram has a prominent central fuzzy spot, due to the directionally reflecting lower lamina, plus wide-field-scattered, orange light coming from the other scale components.

Figure 4 does not include a cream-coloured scale, because it appeared to be an intermediate case of the white and orange scales. Similarly, the data obtained with brown scales resembled those of the black scales.

The scatterograms show that butterfly wing scales are complex optical systems. With normal illumination, that is, from the upper, abwing side, light diffraction by the array of ridges in the upper lamina is always present. Indeed, diffraction by the array of parallel ridges of the scales' upper lamina is universally observed in butterfly scales (Giraldo 2008; Kinoshita 2008). Wide-field light scattering is

especially prominent in the pigmented scales, and thin-film reflection is dominant in the blue scales. Thin-film reflection also occurs in black and brown scales, but the high pigment absorbance effectively prevents its contribution to colouration. The blue scales also have a considerable amount of melanin, even substantially higher than that in the brown scales (Fig. 2b), and, therefore, the contribution of the blue scales' lower lamina to the reflected light signal is minor, like in the brown scales. In other words, the reflectance of the blue scale measured with normal, abwing illumination will be virtually exclusively determined by the reflecting upper lamina. This conclusion is underscored by the absence of a fuzzy spot in the abwing scatterogram, which only shows a narrow diffraction pattern (Fig. 4a).

Thin films

The combination of pigments and structures determine the colours displayed by the wing scales of *B. philenor*. Of primary importance is, of course, the main material of the butterfly wing scales, chitin. We previously studied the glass scales of another papilionid butterfly, *Graphium sarpedon* (Stavenga et al. 2012b). These scales are unique, since trabeculae are missing and the upper and lower lamina, each with thickness ~ 200 nm, are collapsed, together approximating a single cuticular plate with thickness ~ 400 nm. The glass scales allowed the measurement of the refractive index throughout the visible wavelength range, being about 1.55, with a minor, normal dispersion (Fig. 5a, from Leertouwer et al. 2011). The absorption spectrum of the scales' chitin could only be measured with our microspectrophotometer at wavelengths >350 nm and, therefore, we measured the absorption coefficient of a piece of cicada wing (Fig. 5a). The cicada's chitin absorbs in the far-ultraviolet, with a distinct peak at ~ 280 nm (Stoddart et al. 2006). The absorption peak fully corresponds with the reflectance minimum of the white areas in the ventral hindwings (Fig. 1c, #1).

The reflectance measurements and scatterometry of the adwing side of the scales demonstrated that the lower lamina acts as a thin film (Fig. 4). Using the refractive index of the glass scales of *G. sarpedon*, we calculated the reflectance spectra for three thin films, with thickness 160, 200, and 240 nm (Fig. 5b). We distinguished two cases. First, we neglected the cuticle absorption, which yielded the dashed spectra of Fig. 5b. Second, we included the chitin absorption, which yielded the continuous curves (Fig. 5b). The calculated reflectance spectra have 150–200 nm wide bands, with peak reflectances only slightly depending on dispersion and absorption; the wavelength position of the extrema strongly depends on the film thickness, however. Concerning shape and bandwidths, the calculated spectra resemble the oscillating reflectance spectra measured from

single, isolated scales, but the extrema of the reflectance spectra measured from the different scales did not all have the same wavelength position. This indicates that the thickness of the scales' lower lamina varies (Fig. 4). The thin film thickness of the black (Fig. 4b) and white (Fig. 4c) scales appears to be <200 nm, and especially for the orange scales (Fig. 4d), the reflectance spectra suggest values <160 nm. A smaller thickness of the orange scales may have special functional relevance, because the reflectance is then high in the long wavelength range, that is, where the orange scale's pigment no longer absorbs. The lower lamina thus can noticeably contribute to the total scale reflection.

The reflectance spectra measured from the two sides of the blue scale are very similar (Fig. 4a). Thin-film theory yields for a thin film with thickness 220 nm and the refractive index of an unpigmented butterfly scale a blue-peaking reflectance spectrum (Fig. 5c, cuticle—blue curve). However, the blue scales contain a substantial amount of melanin pigment (Fig. 2b), which must be taken into account. Assuming that the melanin is equally distributed in the two laminae yields a reduced reflectance for the same thin film (Fig. 5c, melanin—cyan curve). Yet, highly concentrated melanin in a very thin layer can cause a substantial increase of the refractive index, from 1.6 up to 1.8 (Stavenga et al. 2012a). Assuming such a refractive index increase not only causes an increased reflectance, but also shifts the reflectance spectrum to distinctly longer wavelengths (Fig. 5c, mel plus—green curve). Still, the blue scale is not a single thin film, but it is in fact a multilayer, consisting of two melanin-pigmented cuticle layers that are separated by a variable air gap (Fig. 5a, inset). We, therefore, calculated the reflectance spectra for 11 cases of two parallel thin films, separated by an air gap varying in steps of $0.1 \mu\text{m}$ between 1.0 and $2.0 \mu\text{m}$. These 3-layer systems yielded strongly oscillating reflectance spectra (Fig. 5c, grey curves; see also Trzeciak et al. 2012). The amplitude of the average reflectance spectrum of the 11 cases is only slightly higher than the amplitude of the spectrum for a single layer (Fig. 5c, 3-layers—red curve). Yet, instead of averaging the reflectance of the 11 individual cases, it may be more appropriate to calculate the square of the average of the electric field amplitudes (Fig. 5c, 3-layers—black curve). That yields a reflectance spectrum that is almost indistinguishable from the one of a single layer. This suggests that the absorbing melanin in the layers in fact optically isolates the lower and upper lamina from each other.

Sexual dichromatism of the dorsal hindwings

Male *B. philenor* have dorsal hindwings with a number of whitish spots in a main, prominent metallic blue-green area (Figs. 1a, 6a). The dorsal hindwings of female feature the

same assembly of spots, but the main area is here brown-black (Fig. 6b; see also Rutowski et al. 2010). Although the male and female dorsal hindwings have strongly different colours, they have similar scale patterns (Fig. 6c, d). Microspectrophotometry of their scales immersed in a refractive index fluid showed very similar melanin pigmentation (Fig. 6c, d, insets) with absorbance spectra virtually identical to those of the blue scales of the ventral hindwings (Fig. 2b). The wing reflectance spectra strongly differ (Fig. 5e), which is probably due to the scales' structure, as indicated by scanning electron microscopy. The abwing surface of the scales at the dorsal hindwings of the male resembles that of the blue scales of the ventral hindwings (Fig. 3e, g), however, with slightly larger windows (not shown), while in the female the dorsal hindwing scales have rather large windows, similar as those of the orange and black scales (as in Fig. 3d). Scales with melanin pigment and large windows illuminated from the abwing side are brown or black (Figs. 1, 2b), but scales with small windows are blue-green iridescent (Figs. 1, 2, 3). In other words, the size of the windows has a crucial effect on the scale's appearance. Like in the blue scales of the ventral hindwings, the upper lamina of the scales of the male dorsal hindwings acts as a thin film reflector, causing a blue-green colour, while the upper lamina of the female scales rather acts as a pigmented diffuser, causing a dull black colour, or, at most a dim iridescence in some females (R. Rutowski, personal communication).

The strong sexual dichromatism of the dorsal hindwings suggests a primary role in intersexual signalling. The male's blue on the dorsal hindwings is known to be a sexual signal (Rutowski and Rajyaguru 2013). During wing movements, the angles of light incidence and reflection, as well as the wing angle with respect to an observer, severely changes, which thus will make the reflectance angle-dependent. Interestingly, because the wings reflect light more or less directionally, polarisation becomes an important aspect. We have, therefore, investigated the angle- and polarisation-dependent reflections of the male's dorsal hindwings (Fig. 7). We mounted a small wing piece at a glass micropipette and measured its light reflection properties with the imaging scatterometer, using a linear-polarised, narrow aperture white light beam ($\sim 5^\circ$). The beam illuminated an area with diameter ~ 0.53 mm (Fig. 7a) from angular directions about 15° , 45° , and 75° with respect to the normal (indicated in the diagram of Fig. 7b by the numbers 1, 2, and 3) with the plane of light incidence approximately parallel to the longitudinal ridges.

If the scales reflected the incident light specularly, the reflected light beams would leave the wing piece under the mirror angle (diagrammatically shown in Fig. 7b by the numbers 1, 2, and 3). This is not precisely the case, as shown by Fig. 7c and d, which present the superimposed

scattering patterns resulting for the three illuminations for TE-(transverse electric- or s-) and TM-(transverse magnetic- or p-)polarised light, respectively. The scatterograms are reminiscent of the diffraction patterns, obtained with local illumination of single scales (Fig. 4), but the patterns are distinctly broadened due to the not perfectly coplanar arrangement of the scales. The centre of the diffraction patterns, located in the plane of light incidence, is at the mirror angle, however. With increasing angle of light incidence, the intensity of the reflected light increases for TE-polarised light, whilst it decreases for TM-polarised light; furthermore, with an increase of the angle of light incidence, the colour of the reflected light shifts towards shorter wavelengths, from blue-green to blue, as expected from thin-film optics (Fig. 7c, d).

The scatterograms of Fig. 7 demonstrate that the reflectance of the male dorsal hindwings strongly depends on polarisation. To investigate this further, we have measured angle-dependent reflectance spectra of a male dorsal hindwing for both TE- and TM-polarised light, using a setup consisting of two rotatable optical fibres connected to a spectrometer. The light beam's incident plane was again along the longitudinal ridges of the scales (approximately corresponding to the vertical coordinate of Fig. 7c, d), and the light-collecting optical fibre was rotated in the same plane until the signal was maximal; the fibre's angular position where the reflection signal was maximal was found to be always virtually identical to the mirror angle.

At normal incidence, the peak reflectance was ~ 500 nm, but with increasing angle of incidence the peak wavelength was blue shifted for both TE- and TM-polarised light (Fig. 8a–c). The angle-dependence of the reflectance amplitude was quite different for both cases, however (Fig. 8a, b, d). With increasing angle of incidence, the peak amplitude monotonically increased for TE-polarised light, but for TM-polarised light, the amplitude first decreased, became minimal between 50° and 60° , and increased again for larger angles.

Modelling of the angle-dependent reflectance spectra for a single thin film closely resembled the experimental curves, but perfect correspondences could not be obtained, most probably because of the variations in scale structure and scale arrangement on the wing. Nevertheless, both calculated and experimental spectra demonstrated strongly polarised light reflections at oblique illuminations.

Discussion

Pigments

The wing scales of *B. philenor* contain various pigments. The white scales appear to be non-pigmented with only

chitin present. The cream-coloured scales probably contain papiliochrome II, which absorbs distinctly in the ultraviolet only, while the pigment in the orange scales absorbs as well in the blue wavelength range (Fig. 2a). The latter pigment's absorbance spectrum is very similar to that of the pigment in the orange spots that exists on both dorsal and ventral wings of *P. xuthus* (Wilts 2013). Presumably, this pigment is an as yet uncharacterised papiliochrome.

The prominent element of the brown, blue and black scales is melanin pigment, with a broad absorption range, extending from the ultraviolet into the infrared (Fig. 2b). We previously found that the absorbance spectrum of the melanin of damselfly wings could be well fitted with an exponential function $D = D_0 \exp(-\lambda/\lambda_m)$, yielding a value $\lambda_m = 175$ nm, corresponding to that describing the spectrum of vertebrate eumelanin (Stavenga et al. 2012a). Fitting an exponential to the melanin spectra of *B. philenor* yielded much larger values, $\lambda_m = 250$ – 300 nm, however, indicating that the melanin absorbance spectrum is species dependent.

Thin films

An important finding of the present study is that a scale's colour not only depends on the specific pigment and its concentration, but also on the lower lamina's thin film characteristics. Furthermore, pigment and thin film seem to be spectrally tuned. For *B. philenor*, this is most apparent in the orange scales. The transmittance of the pigment in the upper lamina is low in the short-wavelength range and high at longer wavelengths, and the reflectance of the lower lamina's thin film has the same spectral properties. In the unpigmented white scales, the diffusive upper lamina and lower lamina's thin film jointly cause a broad-band reflectance spectrum. In the black scales, the lower lamina strongly reflects in the blue wavelength range, but the heavily pigmented upper lamina most effectively suppresses this reflection because of the higher melanin absorption at shorter wavelengths. The situation is different in the blue scales, where both lower and upper lamina act as thin films with maximal reflection in the blue wavelength range (Fig. 4a). Modelling yields that for abwing illumination, the upper lamina determines the reflectance (Fig. 5c). We may speculate that a possible reason for the melanisation of the blue scales is to optimise polarisation. In case both the upper and lower lamina can contribute to the scale reflectance, the light fraction that is reflected by the lower lamina may become depolarised when it has traversed twice the upper lamina and the trabeculae. Oblique illumination will then not yield a strong polarisation signal as is the case with only a single reflecting layer.

Diffraction

All scales, when illuminated at the abwing side with a point source, show a distinct diffraction pattern, which is created by the array of parallel ridges. Especially the diffraction pattern of the white scales is colourful (Fig. 4c). In the scales with papiliochromes, the diffracted light is spectrally filtered, which causes a cream or orange colour (Fig. 4d). In the brown and black scales, substantial absorption of the incident light by melanin severely reduces the reflection, so that documenting a clear diffraction pattern required a prolonged exposure (Fig. 4b). The diffraction patterns vanish, however, with an increase of the aperture of the illuminating light source and/or increase of the illumination area, resulting in a diffuse colour.

Sexual dichromatism

The coloured scale patterns displayed on the dorsal and ventral sides of the wings of butterflies very often differ distinctly, indicating their different biological functions. For instance the peacock, *Aglais io*, a nymphalid, has colourful dorsal wings, with prominent eyespots, presumably functioning in scaring away predatory birds (Blest 1957). The peacock's ventral wings are on the contrary a very inconspicuous dull brown, creating a perfect camouflage of the butterfly in a cluttered environment when at rest. The situation is very different in the case of the Pipevine Swallowtail, *B. philenor*. Here, the ventral hindwings of both the male and female have a very conspicuous patterning. The display of the hindwings is quite effective in signalling the unpalatability of *B. philenor* butterflies (Brower 1958; Pegram et al. 2013a, b). *B. philenor* is in the centre of a Batesian mimicry complex, so that a number of non-toxic butterfly species with similar wing patterns is less vulnerable for predation (Brower 1958; Brower and Brower 1962; Prudic and Oliver 2008).

The scales on the dorsal hindwings of male and female of *B. philenor* contain about the same amount of melanin (Fig. 6c, d, insets), but the virtually closed windows of the male's scales vs the much wider windows of the female's scales cause the dramatically different colours: the scales of the male and female are distinctly iridescent and dull brown-black, respectively (Figs. 6, 7), suggesting that the iridescence of the male's dorsal hindwings functions in intersexual signalling (Kemp and Rutowski 2011; Rajyaguru et al. 2013). During flight and during the male's courtship behaviour, the moving wings cause a continuously changing angle of observation for an expectant observer and thus will cause a continuously changing colour (Rutowski and Rajyaguru 2013). If the set of photoreceptors of *B. philenor* is similar to that of the related papilionid

Papilio xuthus (Arikawa 2003), specifically the violet and blue receptors will detect a strongly varying signal.

With non-normal illuminations of the male dorsal hindwings, the reflected light becomes polarised, with only TE-polarised light remaining at a Brewster's angle of 50°–60° (Figs. 7, 8). Papilionid butterflies can well detect polarised light (Bandai et al. 1992; Kelber et al. 2001; Kinoshita et al. 2011), and thus female *B. philenor* may be able to discriminate the shiny reflections from the males' dorsal hindwings from both the changes in colour and polarisation.

Conclusion

This study shows that the colouration toolkit of *B. philenor* consists of thin films, papiliochrome and melanin pigment. These elements are used in various combinations. Not surprisingly, comparative studies on other butterfly families revealed very similar colouration mechanisms (Stavenga et al. in preparation). Melanin pigments are encountered universally, but nymphaline butterfly wing scales contain, instead of papiliochromes, ommochromes and kynurenine, and the scales of pierids have granules with pterins. Although butterfly scales are known to occur in a wide variety of shapes and colour, the most ubiquitous scale type consists of a flat lower lamina, which acts as an optical thin film, and an upper lamina consisting of ridges and crossribs, which together act as a diffuser. How the tuning of the scales' thin films and pigments is genetically programmed will be an interesting topic for future study.

Acknowledgments We thank Dumas Galvez for collaboration, and Drs Kentaro Arikawa, Helen Ghiradella, Nathan Morehouse and Ronald Rutowski as well as an anonymous referee for valuable comments at the manuscript. This study was financially supported by the Air Force Office of Scientific Research/European Office of Aerospace Research and Development AFOSR/EOARD (grant FA8655-08-1-3012).

References

Arikawa K (2003) Spectral organization of the eye of a butterfly, *Papilio*. *J Comp Physiol A* 189:791–800

Bálint Z, Kertész K, Piszter G, Vértésy Z, Biró LP (2012) The well-tuned blues: the role of structural colours as optical signals in the species recognition of a local butterfly fauna (Lepidoptera: Lycaenidae: Polyommatae). *J R Soc Interface* 9:1745–1756

Bandai K, Arikawa K, Eguchi E (1992) Localization of spectral receptors in the ommatidium of butterfly compound eye determined by polarization sensitivity. *J Comp Physiol A* 171:289–297

Biró LP, Kertész K, Vértésy Z, Márk GI, Bálint Z, Lousse V, Vigneron JP (2007) Living photonic crystals: butterfly scales—nanostructure and optical properties. *Mat Sci Eng C* 27:941–946

Blest AD (1957) The function of eyespot patterns in the Lepidoptera. *Behaviour* 11:209–256

Brower JVZ (1958) Experimental studies of mimicry in some North American butterflies: part II. *Battus philenor* and *Papilio troilus*, *P. polyxenes* and *P. glaucus*. *Evolution* 12:123–136

Brower LP, Brower JVZ (1962) The relative abundance of model and mimic butterflies in natural populations of the *Battus philenor* mimicry complex. *Ecology* 43:154–158

Exner S (1891) *Die Physiologie der facitirten Augen von Krebsen und Insecten*. Deuticke, Leipzig

Ghiradella H (1984) Structure of iridescent lepidopteran scales: variations on several themes. *Ann Entomol Soc Am* 77:637–645

Ghiradella H (1985) Structure and development of iridescent lepidopteran scales: the Papilionidae as a showcase family. *Ann Entomol Soc Am* 78:252–264

Ghiradella H (1998) Hairs, bristles, and scales. In: Locke M (ed) *Microscopic anatomy of invertebrates*, vol 11A., Insecta. Wiley, New York, pp 257–287

Ghiradella H (2010) Insect cuticular surface modifications: scales and other structural formations. *Adv Insect Physiol* 38:135–180

Ghiradella H, Aneshansley D, Eisner T, Silberglied R, Hinton HE (1972) Ultraviolet reflection of a male butterfly: interference color caused by thin-layer elaboration of wing scales. *Science* 178:1214–1217

Giraldo MA (2008) *Butterfly wing scales: pigmentation and structural properties*. Thesis, Groningen

Hooke R (1665) *Micrographia or some physiological descriptions of minute bodies made by magnifying glasses*. J. Martyn, J. Allestry, London

Ingram AL, Parker AR (2008) A review of the diversity and evolution of photonic structures in butterflies, incorporating the work of John Huxley (The Natural History Museum, London from 1961 to 1990). *Phil Trans R Soc B* 363:2465–2480

Kelber A, Thunell C, Arikawa K (2001) Polarisation-dependent colour vision in *Papilio* butterflies. *J Exp Biol* 204:2469–2480

Kemp DJ, Rutowski RL (2011) The role of coloration in mate choice and sexual interactions in butterflies. *Adv Stud Behav* 43:55–92

Kinoshita S (2008) *Structural colors in the realm of nature*. World Scientific, Singapore

Kinoshita M, Shimada N, Arikawa K (1999) Colour vision of the foraging yellow swallowtail butterfly *Papilio xuthus*. *J Exp Biol* 202:95–102

Kinoshita S, Yoshioka S, Kawagoe K (2002) Mechanisms of structural colour in the *Morpho* butterfly: cooperation of regularity and irregularity in an iridescent scale. *Proc R Soc Lond B* 269:1417–1421

Kinoshita S, Yoshioka S, Miyazaki J (2008) Physics of structural colors. *Rep Prog Phys* 71:076401

Kinoshita M, Yamazato K, Arikawa K (2011) Polarization-based brightness discrimination in the foraging butterfly, *Papilio xuthus*. *Phil Trans R Soc B* 366:688–696

Koch PB, Behnecke B (2000) The molecular basis of melanism and mimicry in a swallowtail butterfly. *Curr Biol* 10:591–594

Koshitaka H, Kinoshita M, Vorobyev M, Arikawa K (2008) Tetrachromacy in a butterfly that has eight varieties of spectral receptors. *Proc R Soc B* 275:947–954

Leertouwer HL, Wilts BD, Stavenga DG (2011) Refractive index and dispersion of butterfly scale chitin and bird feather keratin measured by interference microscopy. *Opt Express* 19:24061–24066

Mason CW (1924) Blue eyes. *J Phys Chem* 28:498–501

Menzel R, Backhaus WGK (1989) Color vision of honey bees: phenomena and physiological mechanisms. In: Stavenga DG, Hardie RC (eds) *Facets of vision*. Springer, Berlin, pp 281–297

Michielsen K, Stavenga DG (2008) Gyroid cuticular structures in butterfly wing scales: biological photonic crystals. *J R Soc Interface* 5:85–94

Michielsen K, De Raedt H, Stavenga DG (2010) Reflectivity of the gyroid biophotonic crystals in the ventral wing scales of the

- Green Hairstreak butterfly, *Callophrys rubi*. J R Soc Interface 7:765–771
- Morehouse NI, Vukusic P, Rutowski R (2007) Pterin pigment granules are responsible for both broadband light scattering and wavelength selective absorption in the wing scales of pierid butterflies. Proc R Soc B 274:359–366
- Nijhout HF (1991) The development and evolution of butterfly wing patterns. Smithsonian Institution Press, Washington
- Nijhout HF (1997) Ommochrome pigmentation of the *linea* and *rosa* seasonal forms of *Precis coenia* (Lepidoptera: Nymphalidae). Arch Insect Biochem Physiol 36:215–222
- Pegram KV, Lillo MJ, Rutowski RL (2013a) Iridescent blue and orange components contribute to the recognition of a multicomponent warning signal. Behaviour 150:321–336
- Pegram KV, Nahm AC, Rutowski RL (2013b) Warning color changes in response to food deprivation in the pipevine swallowtail butterfly, *Battus philenor*. J Insect Sci 13:1–16
- Pirih P, Wilts BD, Stavenga DG (2011) Spatial reflection patterns of iridescent pierid butterfly wings and the dependence of visibility on scale curvature. J Comp Physiol A 197:987–997
- Prudic KL, Oliver JC (2008) Once a Batesian mimic, not always a Batesian mimic: mimic reverts back to ancestral phenotype when the model is absent. Proc R Soc B 275:1125–1132
- Rajyaguru PK, Pegram KV, Kingston AC, Rutowski RL (2013) Male wing color properties predict the size of nuptial gifts given during mating in the Pipevine Swallowtail butterfly (*Battus philenor*). Naturwissenschaften 100:507–513
- Reed RD, Nagy LM (2005) Evolutionary redeployment of a biosynthetic module: expression of eye pigment genes vermilion, cinnabar, and white in butterfly wing development. Evol Dev 7:301–311
- Rutowski RL, Rajyaguru PK (2013) Male-specific iridescent coloration in the Pipevine Swallowtail (*Battus philenor*) is used in mate choice by females but not sexual discrimination by males. J Insect Behav 26:200–211
- Rutowski RL, Macedonia JM, Morehouse N, Taylor-Taft L (2005) Pterin pigments amplify iridescent ultraviolet signal in males of the orange sulphur butterfly, *Colias eurytheme*. Proc R Soc B 272:2329–2335
- Rutowski RL, Macedonia JM, Merry JW, Morehouse N, Yturralde K, Taylor-Taft L, Gaalema D, Kemp DJ, Papke RS (2007) Iridescent ultraviolet signal in the orange sulphur butterfly (*Colias eurytheme*): spatial, temporal and spectral properties. Biol J Linn Soc 90:349–364
- Rutowski RL, Nahm AC, Macedonia JM (2010) Iridescent hindwing patches in the Pipevine Swallowtail: differences in dorsal and ventral surfaces relate to signal function and context. Funct Ecol 24:767–775
- Srinivasarao M (1999) Nano-optics in the biological world: beetles, butterflies, birds and moths. Chem Rev 99:1935–1961
- Stavenga DG, Stowe S, Siebke K, Zeil J, Arikawa K (2004) Butterfly wing colours: scale beads make white pierid wings brighter. Proc R Soc Lond B 271:1577–1584
- Stavenga DG, Giraldo MA, Hoenders BJ (2006) Reflectance and transmittance of light scattering scales stacked on the wings of pierid butterflies. Opt Express 14:4880–4890
- Stavenga DG, Leertouwer HL, Pirih P, Wehling MF (2009) Imaging scatterometry of butterfly wing scales. Opt Express 17:193–202
- Stavenga DG, Giraldo M, Leertouwer HL (2010) Butterfly wing colors: glass scales of *Graphium sarpedon* cause polarized iridescence and enhance blue/green pigment coloration of the wing membrane. J Exp Biol 213:1731–1739
- Stavenga DG, Wilts BD, Leertouwer HL, Hariyama T (2011) Polarized iridescence of the multilayered elytra of the Japanese Jewel Beetle, *Chrysochroa fulgidissima*. Phil Trans R Soc B 366:709–723
- Stavenga DG, Leertouwer HL, Hariyama T, De Raedt HA, Wilts BD (2012a) Sexual dichromatism of the damselfly *Calopteryx japonica* caused by a melanin-chitin multilayer in the male wing veins. PLoS One 7:e49743
- Stavenga DG, Mashushita A, Arikawa K, Leertouwer HL, Wilts BD (2012b) Glass scales on the wing of the swordtail butterfly *Graphium sarpedon* act as thin film polarizing reflectors. J Exp Biol 215:657–662
- Stavenga DG, Leertouwer HL, Wilts BD (2013) Quantifying the refractive index dispersion of a pigmented biological tissue using Jamin-Lebedeff interference. Light Sci Appl 2:e100
- Stoddart P, Cadusch P, Boyce T, Erasmus R, Comins J (2006) Optical properties of chitin: surface-enhanced Raman scattering substrates based on antireflection structures on cicada wings. Nanotechnology 17:680–686
- Sweeney A, Jigging C, Johnsen S (2003) Polarized light as a butterfly mating signal. Nature 423:31–32
- Tilley RJD, Eliot JN (2002) Scale microstructure and its phylogenetic implications in lycaenid butterflies (Lepidoptera, Lycaenidae). Trans Lepid Soc Japan 53:153–180
- Trzeciak TM, Wilts BD, Stavenga DG, Vukusic P (2012) Variable multilayer reflection together with long-pass filtering pigment determines the wing coloration of papilionid butterflies of the *nireus* group. Opt Express 20:8877–8890
- Umebachi Y (1985) Papiliochrome, a new pigment group of butterfly. Zool Sci 2:163–174
- von Frisch K (1914) Der Farbensinn und Formensinn der Biene. Zool Jb Physiol 35:1–188
- von Frisch K (1949) Die Polarisation des Himmelslichtes als orientierender Faktor bei den Tänzern der Bienen. Experientia 5:142–148
- Vukusic P, Sambles JR (2003) Photonic structures in biology. Nature 424:852–855
- Vukusic P, Stavenga DG (2009) Physical methods for investigating structural colours in biological systems. J R Soc Interface 6:S133–S148
- Vukusic P, Sambles JR, Lawrence CR, Wootton RJ (1999) Quantified interference and diffraction in single *Morpho* butterfly scales. Proc R Soc B 266:1403–1411
- Vukusic P, Sambles JR, Lawrence CR, Wootton RJ (2002) Limited-view iridescence in the butterfly *Ancyluris meliboeus*. Proc R Soc Lond B 269:7–14
- Wijnen B, Leertouwer HL, Stavenga DG (2007) Colors and pterin pigmentation of pierid butterfly wings. J Insect Physiol 53:1206–1217
- Wilts BD (2013) Brilliant biophotonics: physical properties, pigmentary tuning & biological implications. Thesis, Groningen
- Wilts BD, Leertouwer HL, Stavenga DG (2009) Imaging scatterometry and microspectrophotometry of lycaenid butterfly wing scales with perforated multilayers. J R Soc Interface 6:S185–S192
- Wilts BD, Pirih P, Stavenga DG (2011) Spectral reflectance properties of iridescent pierid butterfly wings. J Comp Physiol A 197:693–702
- Wilts BD, Michielsen K, De Raedt H, Stavenga DG (2012a) Iridescence and spectral filtering of the gyroid-type photonic crystals in *Parides sesostris* wing scales. Interface Focus 2:681–687
- Wilts BD, Trzeciak TM, Vukusic P, Stavenga DG (2012b) Papiliochrome II pigment reduces the angle dependency of structural wing coloration in *nireus* group papilionids. J Exp Biol 215:796–805